Dynamic Performance of a Power Conditioner Applied to Photovoltaic Sources

Gabriele GRANDI, Domenico CASADEI, Claudio ROSSI
Dept. of Electrical Engineering - University of Bologna
Viale Risorgimento 2, 40136 - Bologna (Italy)
Tel. +39 051 20 93571, Fax. +39 051 20 93588
http://www.die.ing.unibo.it/

Keywords

Active filters, converter control, energy system management, generation of electrical energy, power conditioning, power quality, renewable energy systems, solar cell systems.

Abstract

A power conditioner connecting a photovoltaic power system to the electrical network is presented and analyzed in this paper. The power conditioner is controlled as an active filter. The stability and the dynamic behavior of the whole system is analyzed by introducing transfer functions. The analytical developments are confirmed by numerical simulations on a realistic circuit model implemented in the Simulink environment of Matlab.

Introduction

Photovoltaic (PV) sources are used today in many specific applications such as battery charging, water pumping, home power supply, swimming-pool heating systems, satellite power systems etc. Furthermore, PV energy seems to become one of the most important renewable energy resources in the near future, since it is clean, pollution free, and inexhaustible.
Despite of these known advantages, the installation cost is still high. In most applications, the generation system requires a dc chopper and a three-phase inverter for the connection to the power grid, as represented in Fig. 1. On the other hand, due to the rapid growth in semiconductors and power electronic techniques, the solar energy is of increasing interest in electrical power applications, and a large research activity has been carried out in this field over the last years [1]-[6].
Since the solar cells still have relatively low conversion efficiency, the use of high efficiency power converters, designed to extract the maximum possible power from the PV module (maximum power point tracking, MPPT) is advisable [1]-[4].
The system considered in this paper (see Fig. 1) is designed to inject into the mains all the available power extracted from the PV cells. In this way, the use of battery or other energy storage devices is avoided, reducing the operating costs and improving the overall system reliability. The considered configuration includes a step-up chopper, a voltage source inverter, a three-phase decoupling inductors

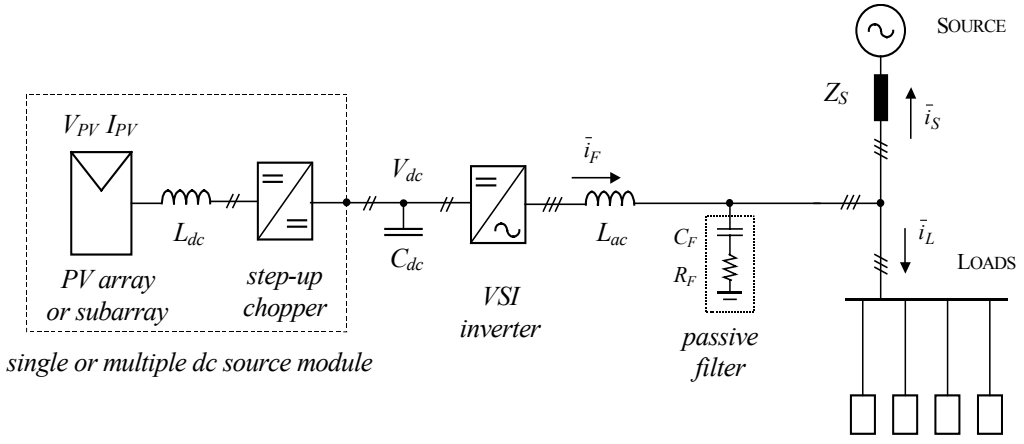

Fig. 1 - Block diagram of the overall PV generation system

and a switch able to disconnect the system in case of power mains failure (islanding prevention). The voltage source inverter, connecting the dc bus to the mains, is controlled such as an active filter. In this way, the system is able to deliver besides the solar power, reactive power and current harmonics in order to compensate non-linear and/or unbalanced loads [7].
The power conditioner, shown in Fig. 1, is able to operate also under unbalanced supply voltages. The proposed control strategy is based on keeping the source currents in phase with the corresponding positive sequence components of the supply voltages. This method leads to sinusoidal balanced source currents, regardless to source voltage unbalance or distortion [8], [9].
A dynamic analysis of the power conditioner in terms of Laplace transform is developed for designing the control system regulators. Numerical simulations are presented for verifying the stability of the system against variations of the generated power and load power, and to show the capability of the power conditioner to operate as active filter.

System Description

a) DC Boost Converter

A photovoltaic cell combines the characteristics of a current source with those of a voltage source. The MPP is located within the operating range, close to the knee of the I/V curve, and it is the preferred working point. However, due to the changes in the environmental variables, i.e., temperature and irradiance, the MPP continuously moves and should be tracked by suitable algorithms in order to obtain optimal system performance [1]-[4].
The power output of a single cell is too low to be useful for power applications, then, several cells are connected in a series/parallel arrangement to form a photovoltaic array, which can deliver the maximum power. In particular, identical PV modules are generally connected in series, in order to obtain a voltage level high enough to realize an efficient dc-dc conversion (the dc-link voltage is usually around 700 V). In this case, the same current flows through each module but the voltage across each module depends on the local environmental parameters. In fact, in addition to the moving shadows caused by the clouds, those created by neighboring buildings and/or trees partially cover some of the PV modules. Then, the MMP condition is not reached for each PV module, and the overall power generated is less than the sum of the maximum power that could be extracted by each module, for the specific environmental parameters of the module.
To avoid this drawback, some authors proposed to divide the array of the PV modules into smaller sub-arrays, each one with its own independent dc-to-dc converter and maximum power controller. Such a scheme allows shaded sub-array to operate close to the MPP, with a reduced power level [5], [6]. On the other hand, multiple dc-to-dc converters lead to lower dc conversion efficiency and reliability, and increasing installation costs.

b) AC Power Conditioner

The aim of the power conditioner is to keep the dc-link capacitor energy E_{dc} close to its reference value E_{dc}^{*}, by properly regulating the current injected into the mains (source current, $\bar{i}_S$), according to the block diagram shown in Fig. 2. In this way, all the power coming from the PV generator is transferred to the electric network.

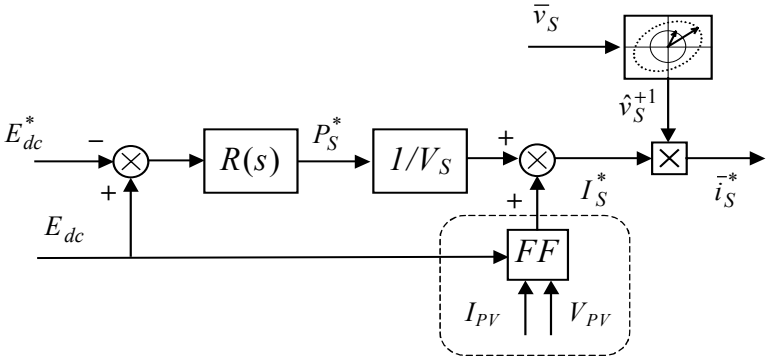

Fig. 2 - DC link energy regulation scheme

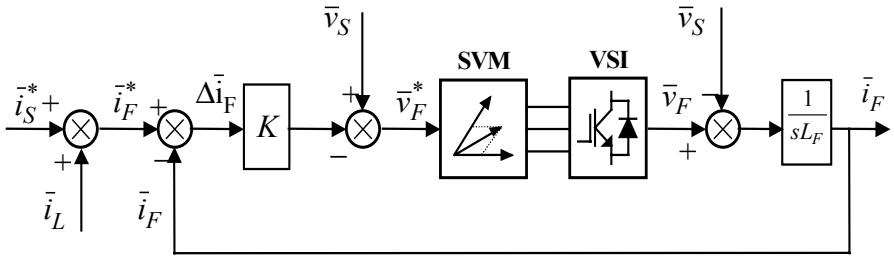

Fig. 3 - Block diagram of the ac current control loop

In particular, the desired amplitude of the source currents, I_S^*, is generated by the regulator $R(s)$, considering the dc-link energy error as input variable. The reference value of the instantaneous source current vector, $\bar{i}_S^*$, is generated on the basis of the magnitude I_S^*, and the phase angle of the positive sequence component of the supply voltages [8], [9], which is represented by the unity space vector $\hat{v}_S^{+1}$ in Fig. 2.

The proposed power conditioning system is also able to compensate non-linear, reactive, pulsating, and/or unbalanced loads [10]. In this case, the ac current control system requires the measurement of both load and filter currents, $\bar{i}_L$ and $\bar{i}_F$ (see Fig.3). The load current is used to calculate the reference value of the filter current $\bar{i}_F^*$, on the basis of the reference source current $\bar{i}_S^*$, given by the dc-link energy regulator, ($\bar{i}_F^* = \bar{i}_S^* - \bar{i}_L$). The measurement of the filter current is used to implement the ac current control loop. A hysteresis current regulator acting on the instantaneous current error $\Delta\bar{i}_F = \bar{i}_F^* - \bar{i}_F$ can be employed to determine the inverter switch states. Alternatively, a PWM (or SVM) current regulator can be used avoiding the drawbacks of hysteresis current controllers. In this case, the reference voltage for the inverter can be calculated by the voltage equation written across the ac-link inductance L, according with the block diagram represented in Fig. 3. Neglecting the resistive effects and introducing a variational model, this equation yields

$$\bar{v}_F^* = \bar{v}_S - \frac{L}{\Delta t}\Delta\bar{i}_F \,. \tag{1}$$

The parameter $L/\Delta t$ in (1) can be adjusted to obtain the desired regulator performance.

Dynamic Analysis

The dynamic behavior of the dc-link controller can be readily analyzed by assuming the energy stored in the dc-link capacitor, E_{dc}, as controlled variable, i.e., by considering $\frac{1}{2}C_{dc}V_{dc}^2$ instead of V_{dc}. In this way, the system behaves as a linear system, and the power flows can be represented in terms of *Laplace* transfer functions [7]. Assuming the power flows as depicted in Fig. 4, the dc-link energy control loop can be represented by the block diagram of Fig. 5.

In order to improve the dynamic behavior of the dc-link voltage controller in response to rapid changes of environmental variables, a feed-forward path (*FF*) could be introduced in the determination of I_S^*, as represented in Fig.2 inside the dashed area. The basic principle is based on the estimation of the instantaneous PV power, $\tilde{P}_{PV}$, in order to predict and consequently compensate the dc-link energy variations. On the other hand, the dynamic of the signal I_S^* should not be too high, in order to ensure sinusoidal source currents and good system performance in terms of power

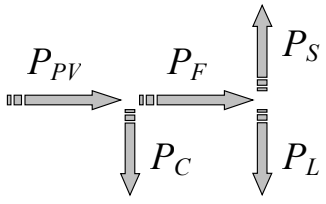

Fig. 4 - Schematic drawing of the power flows

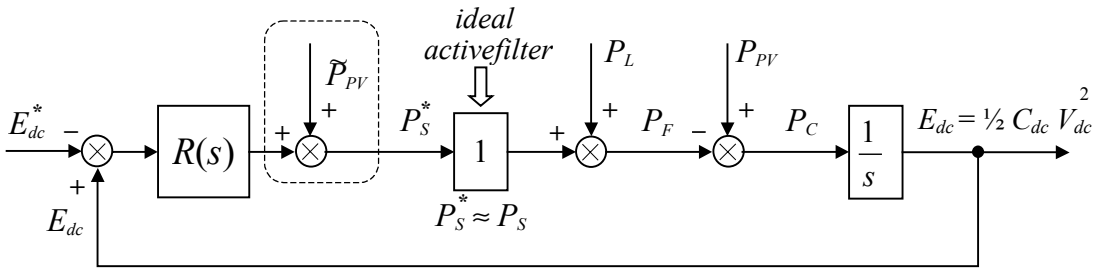

Fig. 5 - Block diagram of the dc-link energy control loop

quality. For this reason, the feed-forward path should be avoided or accurately considered, and the dc-link capacitors should be designed in order to smooth the power fluctuations coming from the PV modules and injected into the mains.

Dc-link Regulator Design Criteria

Considering the block diagram shown in Fig. 5 without the feed-forward compensation block, the source power can be expressed as function of P_{PV}, P_L and E^*_{dc}, leading to

$$P_S = \frac{R(s)}{R(s)+s} P_{PV} - \frac{R(s)}{R(s)+s} P_L - \frac{s\,R(s)}{R(s)+s} E^*_{dc} . \tag{2}$$

This equation shows the influence of photovoltaic or load power variations on the source power. It is interesting to note that the relationship between P_{PV} and P_S is the same of that between P_L and P_S. Basically, the regulator $R(s)$ should be designed for satisfying the source requirements in terms of power quality. Once the regulator $R(s)$ is defined, and the regulator parameters have been tuned to satisfy the desired source power dynamics, the dc-link capacitor should be designed to ensure that the voltage fluctuations during transients would not exceed a prefixed voltage range. The variation of the energy stored in the capacitor can be evaluated from the block diagram shown in Fig. 5 as follows

$$E_{dc} = \frac{1}{R(s)+s} P_{PV} - \frac{1}{R(s)+s} P_L + \frac{R(s)}{R(s)+s} E^*_{dc} . \tag{3}$$

Then, the capacitance C_{dc} can be calculated with reference to the maximum allowed dc-link voltage variation as

$$C_{dc} \geq \frac{2\,\Delta E_{dc}}{\left(V^{max}_{dc}\right)^2 - \left(V^*_{dc}\right)^2}, \text{ where } \Delta E_{dc} = E_{dc} - E^*_{dc} . \tag{4}$$

The transfer functions expressed by (2) and (3) are developed in the following with reference to three types of standard regulators.

a) Proportional Regulator (P)

Assuming for the regulator $R(s)$ a simple proportional gain K_p, leads to

$$R(s) = K_{\mathrm{p}} \tag{5}$$

By introducing (5) in (2) and (3) yields

$$P_S = \frac{1}{1+1/K_p\,s} P_{PV} - \frac{1}{1+1/K_p\,s} P_L - \frac{s}{1+1/K_p\,s} E^*_{dc} , \tag{6}$$

$$E_{dc} = \frac{1}{K_p}\frac{1}{1+1/K_p\,s} P_{PV} - \frac{1}{K_p}\frac{1}{1+1/K_p\,s} P_L + \frac{1}{1+1/K_p\,s} E^*_{dc} . \tag{7}$$

Eq. (6) shows that considering photovoltaic or load power variations, the source power is smoothed with a first-order low-pass filtering action having a time constant $\tau = 1/K_p$.
Eq. (7) shows that a variation in P_{PV} or in P_L leads to a steady-state error in the capacitor energy that is proportional to the time constant $\tau = 1/K_p$.

b) Proportional-Integral Regulator (PI)

Assuming a PI regulator for R(s) leads to

$$R(s) = K_{\mathrm{p}}\left(1+\frac{1}{\tau_i\, s}\right) \tag{8}$$

By introducing (8) in (2) and (3) yields

$$P_S = \frac{(1+\tau_i\, s)\, K_p/\tau_i}{s^2 + K_p\, s + K_p/\tau_i} P_{PV} - \frac{(1+\tau_i\, s)\, K_p/\tau_i}{s^2 + K_p\, s + K_p/\tau_i} P_L - \frac{s\,(1+\tau_i\, s)\, K_p/\tau_i}{s^2 + K_p\, s + K_p/\tau_i} E_{dc}^*, \tag{9}$$

$$E_{dc} = \frac{s}{s^2 + K_p\, s + K_p/\tau_i} P_{PV} - \frac{s}{s^2 + K_p\, s + K_p/\tau_i} P_L + \frac{(1+\tau_i\, s)\, K_p/\tau_i}{s^2 + K_p\, s + K_p/\tau_i} E_{dc}^*. \tag{10}$$

In this case, the transfer functions have a couple of poles. The condition to obtain real poles, i.e. the critical damping, leads to

$$\tau_i = \frac{4}{K_{\mathrm{p}}}. \tag{11}$$

Introducing (11) in (9) and (10) yields

$$P_S = \frac{1+4/K_p\, s}{\left(1+2/K_p\, s\right)^2} P_{PV} - \frac{1+4/K_p\, s}{\left(1+2/K_p\, s\right)^2} P_L - \frac{\left(1+4/K_p\, s\right)s}{\left(1+2/K_p\, s\right)^2} E_{dc}^*, \tag{12}$$

$$E_{dc} = \frac{4}{K_p^2}\frac{s}{\left(1+2/K_p\, s\right)^2} P_{PV} - \frac{4}{K_p^2}\frac{s}{\left(1+2/K_p\, s\right)^2} P_L + \frac{1+4/K_p\, s}{\left(1+2/K_p\, s\right)^2} E_{dc}^*. \tag{13}$$

As it could be expected, (13) shows that there is no steady-state error in the dc-link energy as a consequence of PV or load power variations.

c) Integrating Network (Low-Pass Filter, LPF)

Introducing a real pole in a proportional regulator leads to an integrating network, and the corresponding block behaves as a low-pass filter, leading to

$$R(s) = \frac{K_{\mathrm{p}}}{1+\tau_i\, s}. \tag{14}$$

Introducing (14) in (2) and (3) yields

$$P_S = \frac{K_p/\tau_i}{s^2 + s/\tau_i + K_p/\tau_i} P_{PV} - \frac{K_p/\tau_i}{s^2 + s/\tau_i + K_p/\tau_i} P_L - \frac{s\, K_p/\tau_i}{s^2 + s/\tau_i + K_p/\tau_i} E_{dc}^*, \tag{15}$$

$$E_{dc} = \frac{1}{\tau_i}\frac{1+\tau_i\, s}{s^2 + s/\tau_i + K_p/\tau_i} P_{PV} - \frac{1}{\tau_i}\frac{1+\tau_i\, s}{s^2 + s/\tau_i + K_p/\tau_i} P_L + \frac{K_p/\tau_i}{s^2 + s/\tau_i + K_p/\tau_i} E_{dc}^*. \tag{16}$$

As in the case of a PI regulator, the transfer functions show a couple of poles. The condition to obtain real poles, i.e. the critical damping, leads to

$$\tau_i = \frac{1}{4K_{\mathrm{p}}}. \tag{17}$$

The transfer functions (15) and (16) with the condition expressed by (17) becomes

$$P_S = \frac{1}{\left(1+1/2K_p\,s\right)^2}P_{PV} - \frac{1}{\left(1+1/2K_p\,s\right)^2}P_L - \frac{s}{\left(1+1/2K_p\,s\right)^2}E^*_{dc}, \tag{18}$$

$$E_{dc} = \frac{1}{K_p}\frac{1+1/4K_p\,s}{\left(1+1/2K_p\,s\right)^2}P_{PV} - \frac{1}{K_p}\frac{1+1/4K_p\,s}{\left(1+1/2K_p\,s\right)^2}P_L + \frac{1}{\left(1+1/2K_p\,s\right)^2}E^*_{dc}. \tag{19}$$

As in the case of a proportional regulator, (19) shows that a variation in P_{PV} or in P_L results in a steady-state error in the capacitor energy E_{dc} with respect to its reference value E^*_{dc}. Also in this case, the error is proportional to $1/K_p$. This regulator shows better characteristics with respect to the proportional one when the signals are affected by disturbances, i.e., undesired high frequency components. In fact, the integrating action smoothes the high frequencies disturbances, and higher proportional gains can be used.

d) Comparison of the Standard Regulators

In order to compare the behavior of the three standard regulators discussed above, the parameter corresponding to a critical damping have been chosen in both the cases of PI and LPF. Furthermore, the same maximum dc-link energy excursion ΔE_{dc} = 2 kJ has been considered in response to the same PV power step (ΔP_{PV} = 10 kW). In practice, this corresponds to fix the maximum voltage variation at the dc bus during a step change of PV or load power. The source power transient is represented in Fig. 6, the dc-link energy transient is represented in Fig. 7.
Fig. 6 shows that by using the LPF regulator the smoothest transient of P_S is obtained. The PI regulator shows a power overshoot caused by the energy recover from the dc-link capacitor.
Fig. 7 shows that only the PI regulator is able to restore the dc-link reference energy, leading to zero steady-state errors.

Numerical Simulations

A realistic model implemented in the Simulink environment of Matlab has been used to simulate the PV generation system represented in Fig. 1.
The rated power of the photovoltaic system is 10 kW. The dc/dc boost converter connected to the PV array transfers the generated power to the dc-link bus, regardless to the dc-link voltage value.
The dc-link capacitor has a capacitance value C_{dc} = 20 mF. The reference value of the dc-link voltage is V_{dc}* = 700 V. In this way, the energy stored in the dc-link capacitors is high enough to obtain smoothed source power variations, when the PV power and/or the load power suddenly change.
The control of the dc-link capacitor energy and the generation of the reference source current have been implemented according to the scheme of Fig. 2. Then, the instantaneous value of the reference filter current $\vec{i}^*_F$ is determined as represented in the scheme of Fig.3. The voltage source inverter is controlled by a Space Vector Modulation (SVM) technique, using a carrier frequency of 10 KHz.
The three-phase ac line inductor parameters are L_{ac} = 2 mH, R_{ac} = 0.1 Ω. Ideal sinusoidal source voltages (380 V, 50 Hz) have been assumed during the system operation.
The numerical results of all simulations have been obtained using the same control parameters. In particular, with reference to the control scheme of Fig. 2, a simple proportional regulator $R(s) = K_p = 8$ has been chosen to control the dc-link energy.
The performance of the power conditioning system connected to the photovoltaic array has been evaluated in both steady-state and transient operating conditions.

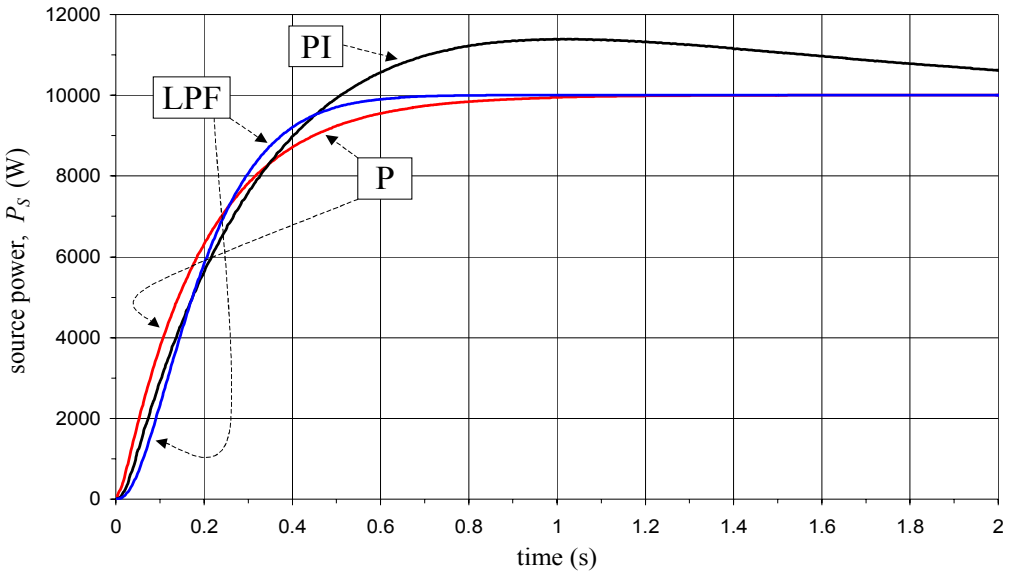

Fig. 6 - Source power transients corresponding to a PV power step of 10 kW

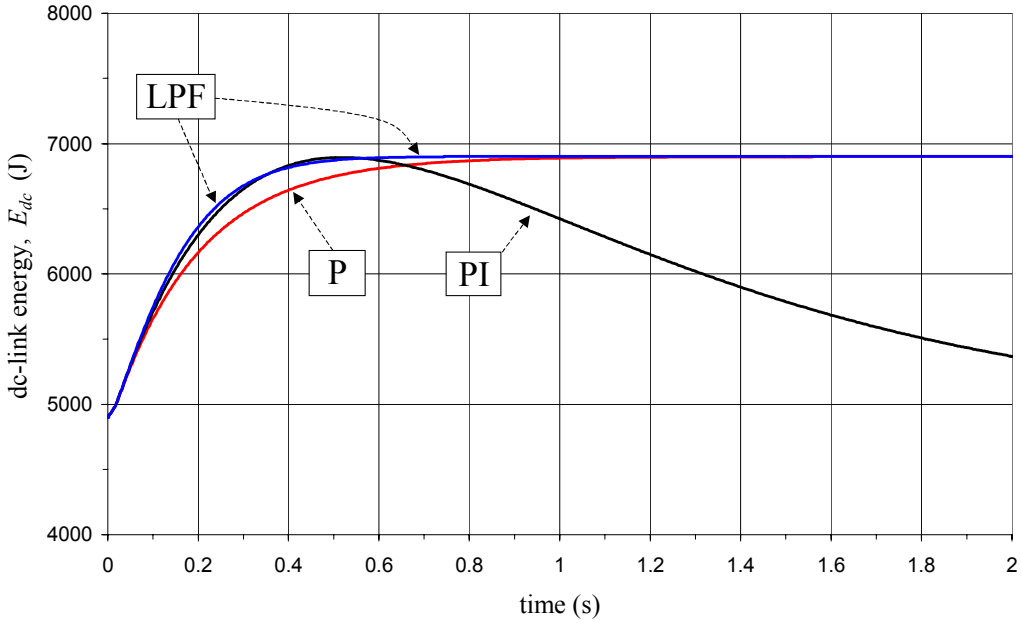

Fig. 7 - Dc-link energy transients corresponding to a PV power step of 10 kW

Fig. 8 depicts the behaviour of the PCS for idealized step variations of the PV power, with a three-phase R-L load (P = 2 kW, cos φ = 0.8) permanently connected to the mains. At the beginning of the simulation, the PV array is disconnected and the PCS operates as active power filter, compensating the reactive power of the load. The dc-link voltage reaches a steady-state value of 680 V. At time t = 1 s the PV array is connected, generating the rated power of 10 kW. The power flows into the dc-link determining a transient in the capacitor energy and in the source power. The source does not receive instantaneously the full-generated PV power, but only an increasing percentage, being the remaining amount stored in the dc-link capacitors. The steady-state value of the source power is reached 0.5 s after the connection of the PV array, and it is equal to the difference between the generated PV power and the power supplied to the load. In these operating conditions the steady-state value of the dc-link voltage is 770 V. At time t = 1.5 s the PV generated power is reduced to the 50% of the rated value (i.e., 5 kW). The corresponding source power variation is smoothed by the PCS by exploiting a fraction of the energy stored in the dc-link capacitor.

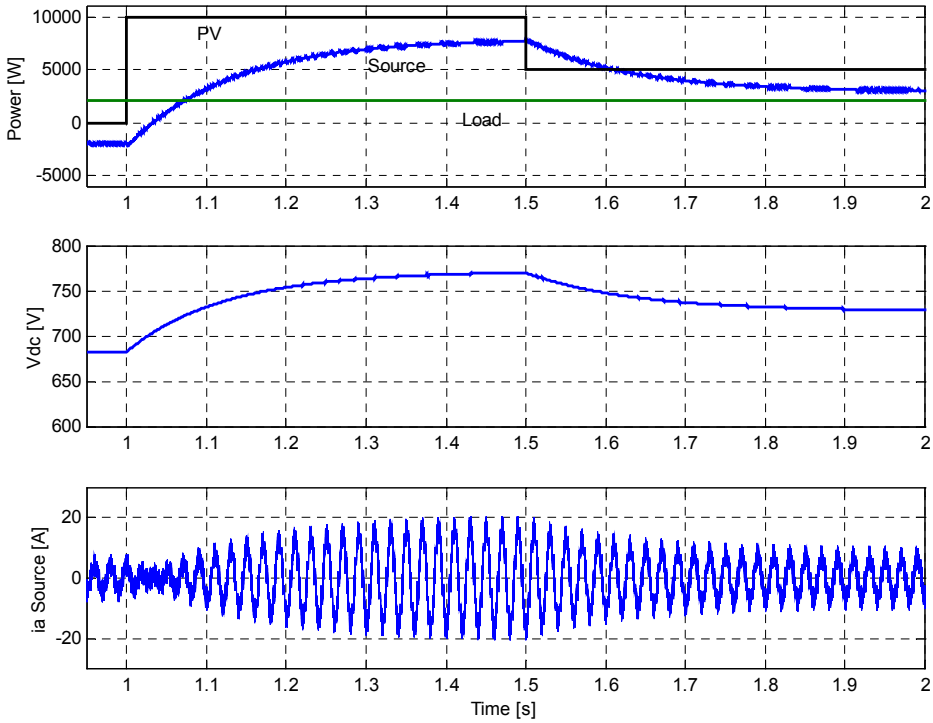

Fig. 8 - Response of the PCS to step variations of the PV generated power

Fig. 9 depicts the behaviour of the PCS for step variations of the load power (a switch-on and -off cycle). In this case the three-phase R-L load is characterized by the following parameters: P = 7 kW, cos φ = 0.6. The power generated by the PV array is assumed constant and equals to the rated value (10 kW). At the beginning of the simulation, the load is switched off, and the PCS transfers the whole power generated by the PV array into the mains. In this condition, the dc-link voltage reaches a steady-state value of 780 V. At time *t* = 0.5 s the load is switched on determining a transient in the dc-link voltage and in the source power. At time t = 1 s the load is switched off. As shown in Fig. 9, the source

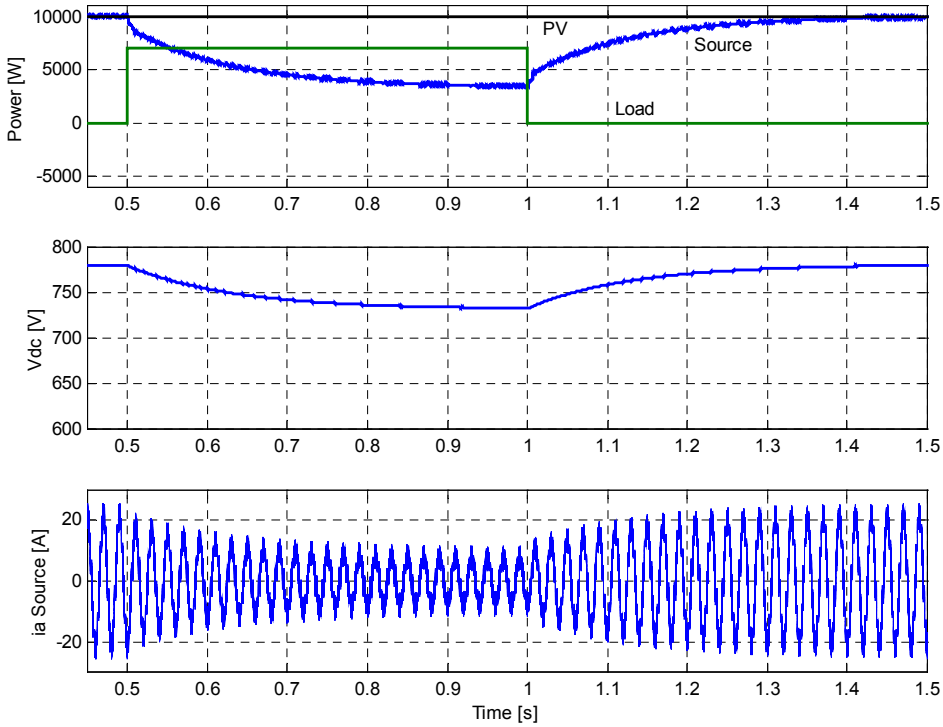

Fig. 9 - Response of the PCS to step variations of the load power

It should be noted that the smoothing effects on the source power introduced by the PCS is a very important feature aimed to avoid perturbations on the electric network caused by step variations of injected or absorbed power.
Figs.10 and 11 have been obtained expanding the time scale of Fig. 9 around the time instant t=0.5s and t=1s, respectively. In this way it is possible to better emphasize the behaviour of the PCS operating as active filter. In particular, it can be noted that the source current is exactly in phase with the source voltage before, during and after the switching-on and -off transients. This means that the proposed

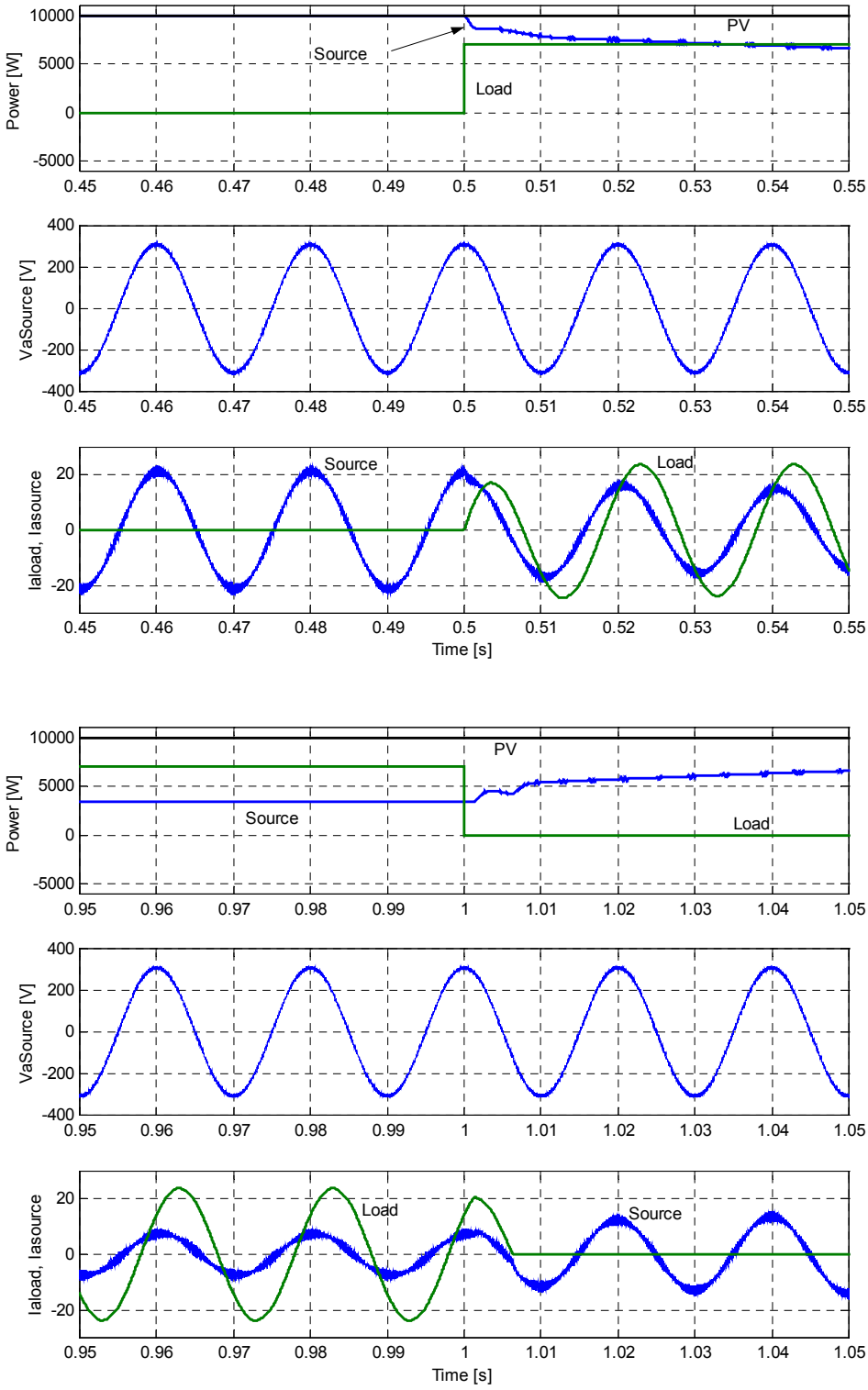

Fig. 11 - Compensation of the load reactive power during the switching-off of the load

Conclusion

In this paper a photovoltaic generation system designed for injecting into the mains the power extracted from the PV array and to perform additional tasks has been analyzed.
The PV array is connected to the dc bus by a dc/dc chopper to maximize the output power. The proposed ac power conditioner, connecting the dc bus to the electrical network, is controlled such as an active filter. In this way, the system is able to deliver the solar power, and also reactive power and current harmonics, in order to compensate non-linear and/or unbalanced loads.
A detailed dynamic analysis of the dc-link energy regulator is carried out with reference to three types of regulators emphasizing the basic features of each one.
Numerical simulations of the whole PV generating system in both steady state and transient operating conditions have been presented. The obtained results show the capability of the system to smooth the source power variations due to step changes of the power generated by the PV array or the power absorbed by the load. The capability of the system to operate as active filter has been also verified.
The proposed PCS configuration can be considered as a viable solution for the better exploitation of the solar energy, complying with the power quality requirements These combined features allow to decrease the operating costs and to improve the overall system efficiency.

References

[1] Y.C. Kuo, T.J. Liang, J.F. Chen, "Novel maximum-power-point-tracking controller for photovoltaic energy conversion system," *IEEE Trans. on Industrial Electronics*, Vol. 48 No. 3, June 2001, pp. 594-601

[2] J.A.M. Bleijs, J.A. Gow, "Fast maximum power point control of current-fed DC-DC converter for photovoltaic arrays," *Electronics Letters*, Vol. 37, N. 1, 4 Jan. 2001, pp. 5-6

[3] T.Y. Kim, H.G. Ahn, S.K. Park, Y.K. Lee, "A novel maximum power point tracking control for photovoltaic power system under rapidly changing solar radiation," *Proc. of IEEE International Symposium on Industrial Electronics*, ISIE 2001, Pusan, Korea, Vol. 2, pp. 1011-1014

[4] J.A. Gow, C.D. Manning, "Controller arrangement for boost converter systems sourced from solar photovoltaic arrays or other maximum power sources," *IEE Proceedings of Electric Power Applications*, Vol. 147, No. 1, Jan. 2000, pp. 15-20

[5] T. Shimizu, M. Hirakata, T. Kamezawa, H. Watanabe, "Generation control circuit for photovoltaic modules," *IEEE Trans. on Power Electronics*, Vol. 16, No. 3, May 2001, pp. 293-300

[6] J.A. Gow, J.A.M. Bleijs, R. Jones, "Optimization of a utility interface for large-scale photovoltaic power systems," *Proc. of European Power Electronic Conference*, EPE 2001, Gratz (Austria) September 2001

[7] D. Casadei, G. Grandi, U. Reggiani, G. Serra, "Analysis of a Power Conditioning System for Superconducting Magnetic Energy Storage," *Proc. of IEEE International Symposium on Industrial Electronics*, ISIE, Pretoria (SA), July 7-10, 1998

[8] D. Casadei, G. Grandi, U. Reggiani, G. Serra, A. Tani, "Behavior of a Power Conditioner for μ-SMES Systems under Unbalanced Supply Voltages and Unbalanced Loads," *Proc. of IEEE International Symposium on Industrial Electronics*, ISIE, Bled (SI), July 12-16, 1999

[9] D. Casadei, G. Grandi, C. Rossi, "Effects of Supply Voltage non-Idealities on the Behavior of an Active Power Conditioner for Cogeneration Systems, *Proc. of IEEE Power Electronic Specialist Conference*, PESC, Galway (Ireland), 18-23 June, 2000

[9] D. Casadei, G. Grandi, C. Rossi, "Effects of Supply Voltage non-Idealities on the Behavior of an Active Power Conditioner for Cogeneration Systems, *Proc. of IEEE Power Electronic Specialist Conference*, PESC, Galway (Ireland), 18-23 June, 2000

[10] D. Casadei, G. Grandi, C. Rossi, "A Parallel Power Conditioning System with Energy Storage Capability for Power Quality Improvement in Industrial Plants", European Conference on Power Electronics and Applications, EPE, Graz, Austria, 27-29 August, 2001.